A Mixing-Layer Flow Noise Analysis by Retarded-time Filtering of the Source Field

Florent Margnat

10ème Congrès Français d'Acoustique

Lyon, 12-16 Avril 2010

A mixing-layer flow noise analysis by retarded-time filtering of the source field

Florent Margnat[1]

[1] Arts et Metiers ParisTech, DynFluid, 151 bd de l'Hopital, F-75013 Paris, florent.margnat@paris.ensam.fr

To date, the physical phenomenon that converts kinetic energy into acoustic waves escaping from the flow is not fully understood. Thanks to the increasing computational power, aeroacoustic prediction tools have become more and more fast and accurate. However, it is still challenging to link an acoustic emission pattern to the aerodynamic source field, in terms of causal events. Lighthill's acoustic analogy provides a way to extract the propagative motion from a flow through the expression of source term in an inhomogeneous wave equation. Unfortunately, when the flow is not compact, source field visualisations hardly reveal exact flow locations where the acoustic energy could be produced.
In the present contribution, we study the source field considered at the retarded-time, which is the true radiating quantity. It differs from the fixed-time source field because it takes into account the solution of the wave equation, usually expressed by a Green function. This methodology is applied to a 2D spatially evolving mixing-layer at Re=400 and 0.375 convective Mach number. Areas in the source domain are analysed by evaluating their net contribution to the aeroacoustic integral, and destructive interferences are noticed between non-radiating areas.

1 The Lighthill formalism

Consider the Lighthill equation written as follows with the entropic and viscous terms neglected :

$$\frac{\partial^2 \rho}{\partial t^2} - c_0^2 \Delta\rho \approx \nabla\cdot\nabla\cdot(\rho\mathbf{uu}) = T \qquad (1)$$

The integral solution in free-field gives the acoustic pressure at the observer position $\vec{X}$ and time t as :

$$p_a(\vec{X},t) = \frac{1}{4\pi}\int_{\mathcal{V}} T\left(\vec{x}, t - \frac{|\vec{X}-\vec{x}|}{c_0}\right)\frac{d\vec{x}}{|\vec{X}-\vec{x}|} \qquad (2)$$

where $\vec{x}$ is the position in the source volume $\mathcal{V}$, and c_0 is the sound velocity.

For a compact source volume and/or a far-field observer, the areas where the aeroacoustic source quantity takes significant values can correspond to the true source location. However, it is known that other effects than sound production are contained in T, such as flow effects on sound propagation. Moreover, in the near field and/or for non-compact source volumes, the identification of the source area or quantity which effectively does cause the acoustic signal is not so clear. For such a task, it is better to examine the source term T through the integral solution procedure, which acts like a filter. Thus, the quantity considered in the present study is the field :

$$S_{\vec{X},t}(\vec{x}) = \frac{T\left(\vec{x}, t - \frac{|\vec{X}-\vec{x}|}{c_0}\right)}{4\pi|\vec{X}-\vec{x}|} \qquad (3)$$

for a given observer $\vec{X}$ and some discrete times in its acoustic signal. It is exactly the integrand in (2), and differs from the original T in two ways : the retarded time and the distance attenuation. An evaluation at retarded-time is usually denoted by bracketed expressions.

2 The acoustic emission of a mixing-layer flow

2.1 Flow configuration

The present flow configuration is a two-dimensional spatially evolving mixing-layer, sketched in Figure 1, at Reynolds number $Re = \delta_\omega \Delta U/\nu = 400$, where δ_ω is the vorticty thickness at inflow and $\Delta U = (U_1 - U_2)/c_0$, and Mach numbers $M_1 = 0.5$ and $M_2 = 0.25$. The subscripts 1 and 2 refer to high and low speed flow, respectively.

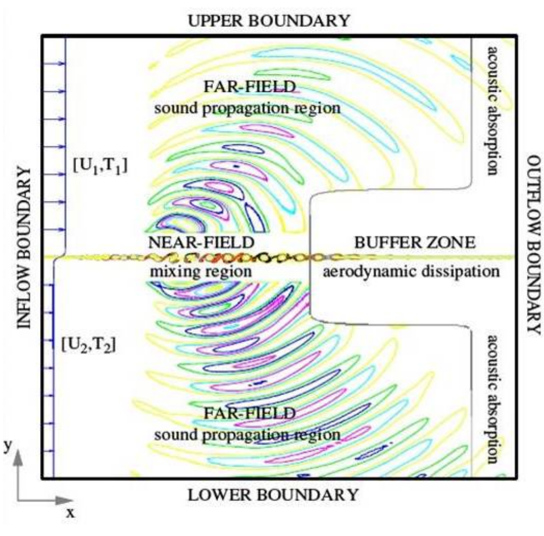

Fig. 1: Flow configuration.

The flow is numerically simulated, with the mixing layer forced at its most unstable frequencies in order to control the roll-up and vortex pairing process. A sponge zone is added to dissipate aerodynamic fluctuations before they reach the outflow boundary and to avoid any spurious reflexion (see Moser *et al.* [2] for more details). The size of the computational domain is $L_x \times L_y = 800\delta_\omega \times 800\delta_\omega$, and the grid resolution is $N_x = 2071 \times N_y = 785$. The cartesian grid is stretched, with the smallest steps near inflow in the flow direction (x), and in the mixing region in the transverse direction (y).

A snapshot of pressure fluctuation in the near-field, with vorticity contours, is plot in Figure 2. The vortex pairing process can be seen around $x/\delta_\omega = 200$, as well as the first wavefronts escaping from the mixing region.

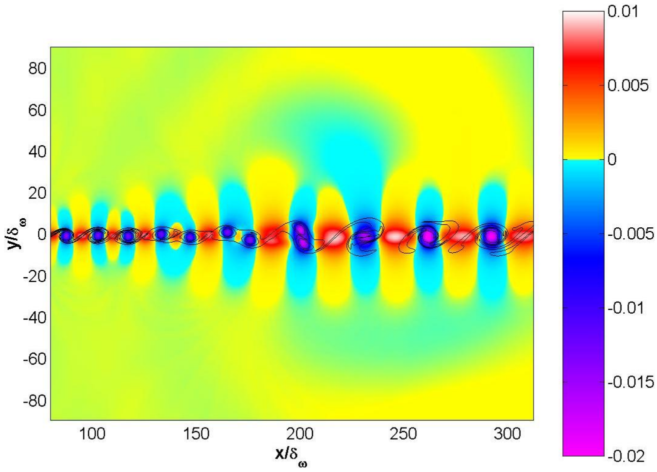

FIG. 2: Mixing-layer flow visualisation. Colorscale : pressure fluctuation ; Lines : vorticity contours.

2.2 Acoustic solution

The obtained database is the input for the computation of the acoustic pressure through the solution (2). The source domain $\mathcal{V}$ is the whole computational domain $L_x \times L_y$ in order to take into account sound-flow interactions which are included in the Lighthill source term, as illustrated by Bogey *et al* [3]. Moreover, only the fluctuating part of the source quantity is used, the mean field being removed in order to compute centered acoustic signals. Finally, weighting functions are applied at the boundaries of the source domain to deal with truncation errors. The obtained acoustic field is plotted in Figure 3. The emission is mainly directed at 35 degrees from the flow axis in the high-speed flow, and at 55 degrees in the low-speed flow.

For the observer point located at $(X/\delta_\omega = 600, Y/\delta_\omega = 300)$, the acoustic signal is plotted in Figure 4. It exhibits a periodic shape at the pairing frequency. Observer times corresponding to maximum, minimum and zero value of this signal will be considered in the following for the source field analysis as defined by (3).

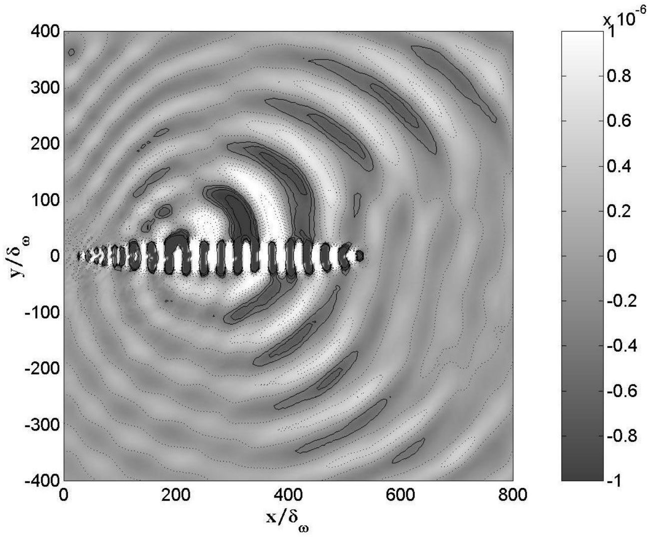

FIG. 3: Acoustic pressure field computed with Lighthill's integral solution.

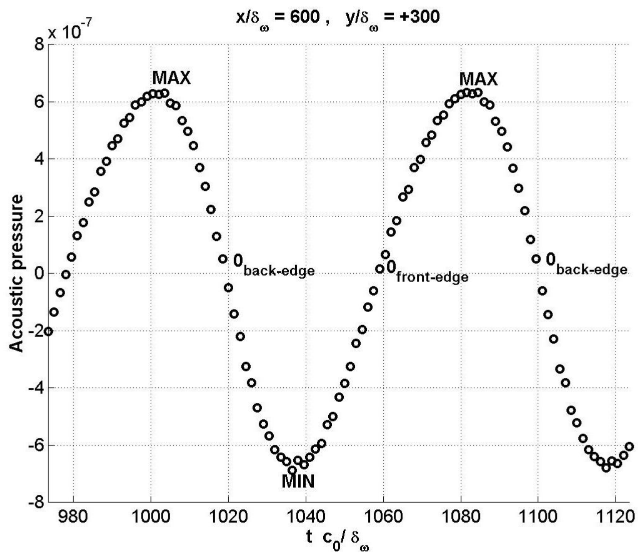

FIG. 4: Acoustic signal at the position $(X/\delta_\omega = 600, Y/\delta_\omega = 300)$.

3 Source field analysis

In this section, the source quantity S is analysed for a fixed observer point located at $\vec{X} = (X = 600\delta_\omega, Y = 300\delta_\omega)$.

3.1 Effect of the retarded time on the source distribution

Firstly, the retarded source field may be compared to the fixed time source field. This is done in Figure 5 along the line $y = 0$ for the time corresponding to the maximum in the acoustic signal. For this comparison, the distance attenuation is not taken into account. Thus the emphasis is put on the modification introduced by the time delay difference between source points. This quantity depends on the Mach number and radiation direction, and is also plotted in Figure 5. The source point

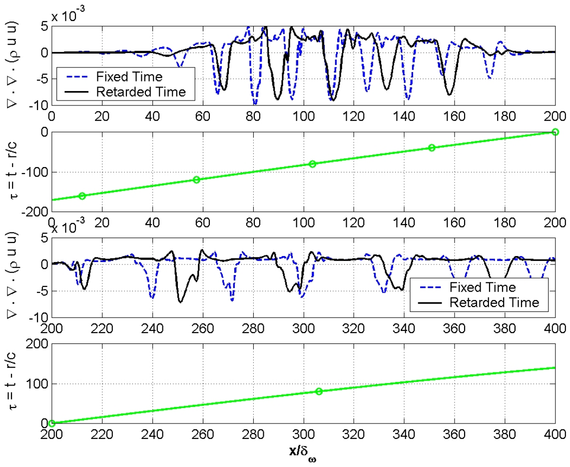

FIG. 5: Evolution of Lighthill's source term and retarded time along x-axis. The observer position is $(X/\delta_\omega = 600, Y/\delta_\omega = 300)$ the observer time t corresponds to the maximum in the acoustic signal.

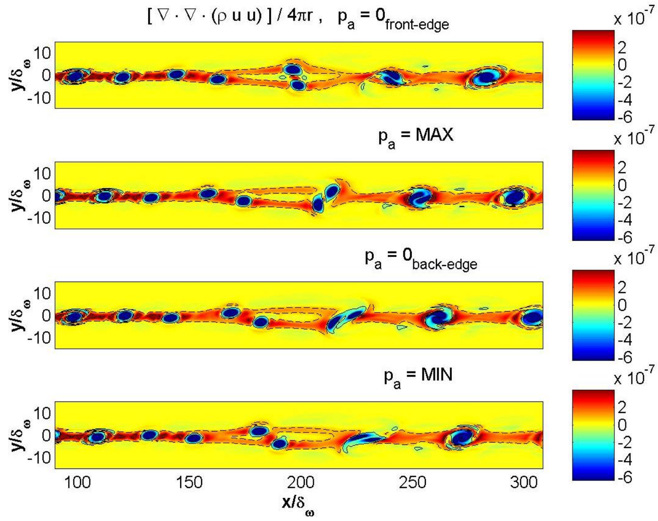

FIG. 6: Source field at retarded times for main acoustic signal events. The observer position is $(X/\delta_\omega = 600, Y/\delta_\omega = 300)$.

$(x/\delta_\omega = 200, y = 0)$ is taken for reference, meaning that it radiates at $\tau = t - r/c = 0$, where $r = |\vec{X} - \vec{x}|$, and the distribution at fixed time is plotted at $\tau = 0$. Naturally, source points upstream from this position must emit before, while source points downstream from this position must emit after. As an indication of the compacity, the positions corresponding to a time delay difference that is a multiple of the rolling or pairing period are also marked. The main observation made from Figure 5 is that the visible wavelength of the vortex street is increased on the retarded time field, because of the global convection movement in the flow.

3.2 Source field in the mixing region

Secondly, source fields at retarded time corresponding to the four main points in the acoustic signal are compared in Figure 6 in the mixing region close to the pairing phenomenon location. Indeed, as shown in Figure 3, acoustic waves seems to originate there. It is very interesting to note that no obvious trend can explain why one field will lead to a maximum of the acoustic signal and the other will lead to a minimum. In other words, noisy events can hardly be extracted from this sequence of vortex-pairing.

Moreover, from both Figures 5 and 6, it appears that a high source amplitude is associated with each vortex or vortex pair, even if no noise seems to come from all of them. Furthermore, on the fields shown in Figure 6, the minima of amplitude are located around $x = 100\delta_\omega$ on the layer axis, while the maxima of amplitude are located around $x = 160\delta_\omega$. It is noteworthy that those locations do not correspond to the apparent source location of the acoustic wavefronts observed in Figure 3, which is located near $x = 200\delta_\omega$. It is also checked that the maximum root-mean-square value of $T(\vec{x})$ occurs around $x = 90\delta_\omega$. These are firm hints about how hard it could be to find true acoustic source location through source field analysis only.

4 The effect of the integration operation

The only missing step between the S-field and the computed acoustic signal is the integration over the source domain. Now, considering the fields in Figure 6, in a vortex peak of radius $2\delta_\omega$ one have $S \approx -4.10^{-7}$. Once integrated, this will result in a contribution to the acoustic signal of about -50.10^{-7}, which is 8 times the signal maximum. However, the mixing-layer exhibits a pattern of highliy coherent positive and negative zones that might balance one another. This is illustrated in Figure 7 and Figure 8. The plotted field of S correponds to the signal maximum $6,4.10^{-7}$ (the integration of the field plotted in Figure 8 over the whole domain does return the value of $6,4.10^{-7}$).

Integration of S over stripes starting inflow gives a contribution of $7,1.10^{-9}$ and $-2,7.10^{-9}$ for zones A and B respectively. Consequently, these are not significant contributions to the integral value. The same conclusion is obtained outflow for well-chosen zones including the whole print of a paired vortex. Those observations confirm a known result, that a vortical structure subjected to convection without deformation does not radiate noise [4].

Also, as expected, the low-speed flow part, zone 2 (see Figure 8), and silent regions in the high-speed flow, zones 3 and 4, have negligible contributions to the signal. More surprising is the total contribution of the layer in the shear region, zone 1, whom integration gives $-1,6.10^{-7}$. This seems to be without intuitive relation with the value on the signal. A similar result is observed for the 3 other selected fields. It is thus shown that the integration over zone 1 of the source quantity S defined by (3) returns values that do not correlate with the corresponding acoustic signal.

However, the signal maximum, minimum and zeros are closely related to the corresponding full fields of S, plotted in figure 9. But the main cause of the signal seems to be located around the observer point. There,

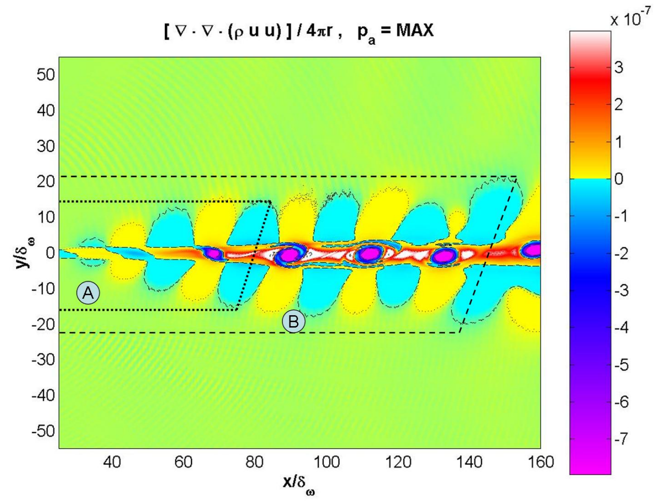

FIG. 7: Source field at retarded time, closeup near inflow. The observer position is $(X/\delta_\omega = 600, Y/\delta_\omega = 300)$, and the observer time corresponds to the maximum in the acoustic signal.

the amplitude of T is 3 orders of magnitude less than in the pairing region, but the distance r is small, resulting in a significant amplitude for S. Moreover, positive and negative zone pattern is visible there too, but spread over larger extents. These two trends may explain why this low-T region is able to contribute significantly to the integral value. So, one can think the signal maximum correspond to the largest positive area of S around the observer point, and conversely for the signal minimum.

5 Conclusions

The present observations showed that over the large source domain considered around a mixing layer, the acoustic pressure signal has not its source at a specific flow event or stress field in the vortex-pairing region, but is rather determined by the vicinity of the observer.

Is that way of thinking a fancy of the mind ? There are some intrinsic limitations of the present analysis : firstly, the observer is inside the source region, thus the analogy assumption of the source - observer separation is violated ; but this separation is between the phenomena : the flow excites the wave equation as an externally applied source term. Thus the acoustic pressure can be computed at an observer located in the source region, provided the acoustic motion does not feedback the flow. Secondly, the integral solution (2) is written for a 3D-case, while our flow is in 2D, where the Green function is slightly different ; but we expect few qualitative influence on the present observations. Finally, what generates the vicinity of the observer is acoustic waves coming from the pairing region, thus it must not be concluded that the pairing phenomenon is silent.

At least, there are two main lessons : on the one hand, a severe warning at interpreting non compact Lighthill's source field distributions as a map of noise sources. On the other hand, we are reminded that acoustics are a branch of fluid dynamics, and that a continous, material propagation medium is required.

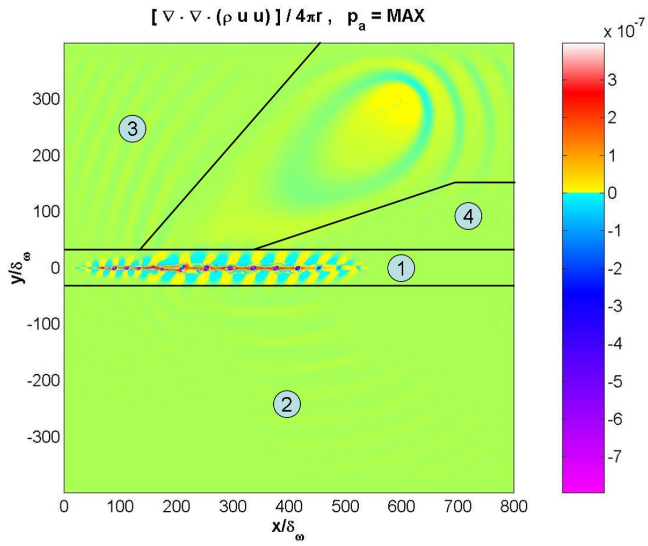

FIG. 8: Source field at retarded time, full source domain. The observer position is $(X/\delta_\omega = 600, Y/\delta_\omega = 300)$, and the observer time corresponds to the maximum in the acoustic signal.

Acknowledgements

The author gratefully acknowledges E. Lamballais and the Laboratoire d'Etudes Aérodynamiques de Poitiers, France, for helpful discussion and the courteous share of the database.

Références

[1] Lighthill M. J., On sound generated aerodynamically. I. General theory, *Proc. Roy. Soc. A*, Vol. 223, pp. 1-32, 1952.

[2] Moser C., Lamballais E. and Gervais Y., Direct computation of the sound generated by isothermal and non-isothermal mixing layers, *12th AIAA/CEAS Aeroacoustics Conference*, AIAA Paper 2006-2447.

[3] Bogey C., Gloerfelt X. and Bailly C., An illustration of the inclusion of sound-flow interactions in Lighthill's equation, *AIAA J.*, 2003 ;41(8) :1604-1606.

[4] Howe M. S., Acoustics of fluid-structure interactions, *Cambridge University Press*, 1998.

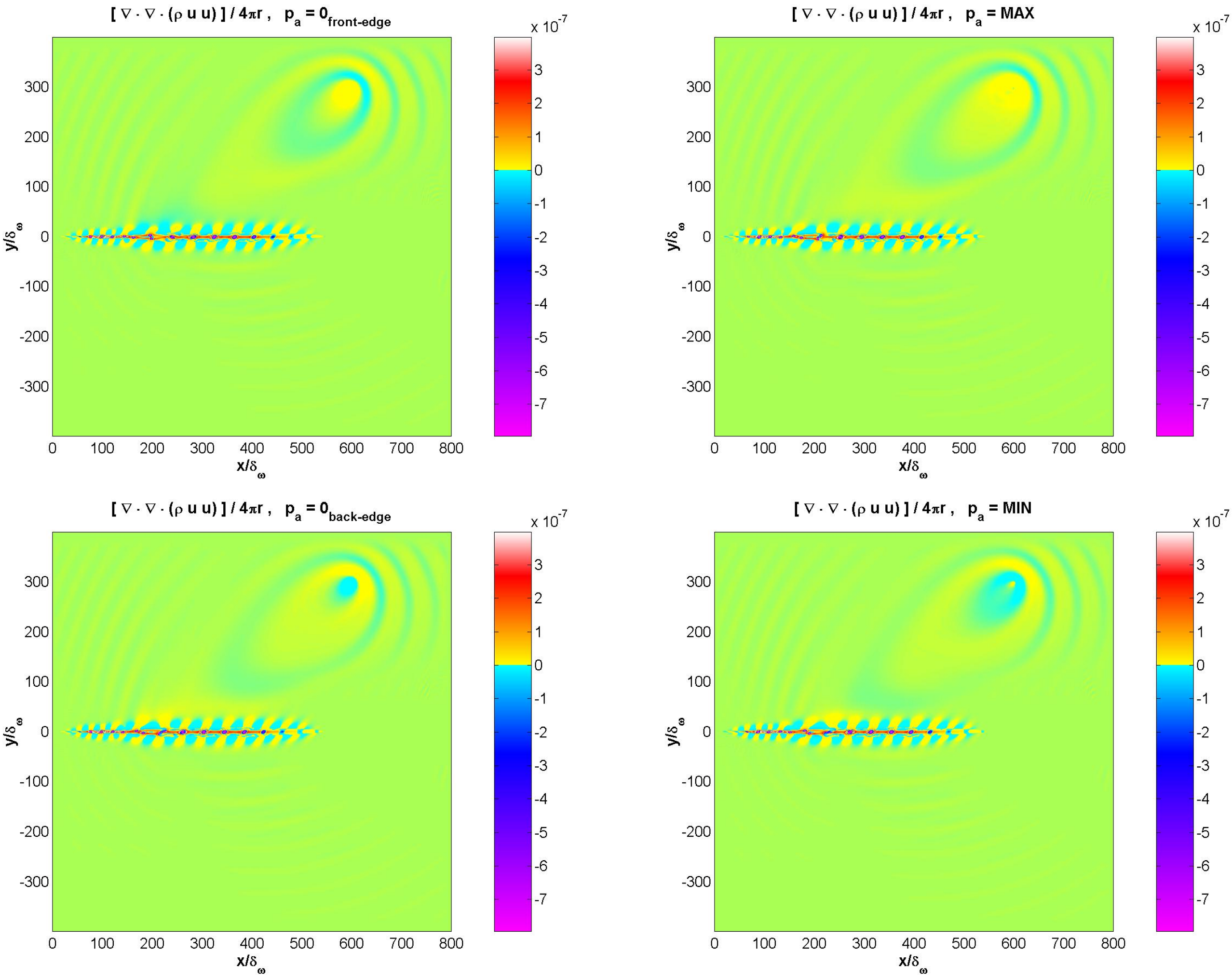

FIG. 9: Source field at retarded times for main acoustic signal events. The observer position is $(X/\delta_\omega = 600, Y/\delta_\omega = 300)$.